Acta Pharmaceutica Sinica B 2020;10(9):1680−1693

Chinese Pharmaceutical Association
Institute of Materia Medica, Chinese Academy of Medical Sciences

Acta Pharmaceutica Sinica B

www.elsevier.com/locate/apsb
www.sciencedirect.com

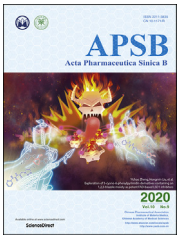

ORIGINAL ARTICLE

Nonclinical safety, tolerance and pharmacodynamics evaluation for meplazumab treating chloroquine-resistant *Plasmodium falciparum*

Kun Zhang[a,b,†], Yu Zhao[b,†], Zheng Zhang[b,†], Mengyao Zhang[b,d], Xiaodong Wu[b,e], Huijie Bian[b,*], Ping Zhu[c,*], Zhinan Chen[a,b,*]

[a]*College of Life Science and Bioengineering, School of Science, Beijing Jiaotong University, Beijing 100044, China*
[b]*National Translational Science Center for Molecular Medicine & Department of Cell Biology, the Fourth Military Medical University, Xi'an 710032, China*
[c]*Department of Clinical Immunology, Xijing Hospital, the Fourth Military Medical University, Xi'an 710032, China*
[d]*Beijing Institute of Biotechnology, Beijing 100071, China*
[e]*Center of Anesthesiology & Operation, Chinese PLA General Hospital, Beijing 100853, China*

Received 27 February 2020; received in revised form 9 June 2020; accepted 16 June 2020

KEY WORDS

Meplazumab;
CD147;
Safety;
Tolerance;
Efficacy;
Nonclinical;
Plasmodium falciparum;
Antimalarial therapy

Abstract Meplazumab is an anti-CD147 humanized IgG2 antibody. The purpose of this study was to characterize the nonclinical safety, tolerance and efficacy evaluation of meplazumab treating chloroquine resistant *Plasmodium falciparum*. Meplazumab was well tolerated in repeat-dose toxicology studies in cynomolgus monkeys. No observed adverse effect level was 12 mg/kg. No difference between genders in the primary toxicokinetic parameters after repeat intravenous injection of meplazumab. No increased levels of drug exposure and drug accumulation were observed in different gender and dose groups. Meplazumab had a low cross-reactivity rate in various tissues and did not cause hemolysis or aggregation of red blood cells. The biodistribution and excretion results indicated that meplazumab was mainly distributed in the plasma, whole blood, and hemocytes, and excreted in the urine. Moreover, meplazumab

Abbreviations: ADA, anti-drug antibody; ADCC, antibody-dependent cell-mediated cytotoxicity; Fab, variable region of monoclonal antibody; Fc, crystalline region of monoclonal antibody; FFPE, formalin-fixed paraffin-embedded; HPLC, high-performance liquid chromatography; HRP, horseradish peroxidase; huRBCs, human red blood cells; IR, inhibition rate; mAbs, monoclonal antibodies; NOG mice, NOD/Shi-scid/IL-2Rγ null mice; Pr, parasitemia; PBS, phosphate buffered saline; PC_{50}, median parasite clearance time; RAP2, rhoptry-associated protein 2; RBCs, red blood cells; RH5, reticulocyte-binding protein homolog 5; RO, receptor occupancy; SD rats, Sprague−Dawley rats; TCA, trichloroacetic acid; WHO, World Health Organization.

*Corresponding authors. Tel: +86 29 84773863.
E-mail addresses: hjbian@fmmu.edu.cn (Huijie Bian), zhuping@fmmu.edu.cn (Ping Zhu), znchen@fmmu.edu.cn (Zhinan Chen).
[†]These authors made equal contributions to this work.

Peer review under the responsibility of Chinese Pharmaceutical Association and Institute of Materia Medica, Chinese Academy of Medical Sciences.

https://doi.org/10.1016/j.apsb.2020.06.011

effectively inhibited the parasites from invading erythrocytes in humanized mice in a time-dependent manner and the efficacy is superior to that of chloroquine. All these studies suggested that meplazumab is safe and well tolerated in cynomolgus monkeys, and effectively inhibits *P. falciparum* from invading into human red blood cells. These nonclinical data facilitated the initiation of an ongoing clinical trial of meplazumab for antimalarial therapy.

1. Introduction

Plasmodium falciparum malaria remains a serious threat to worldwide healthcare. To date, hundreds of millions of malaria cases occur worldwide, most of which are caused by *P. falciparum*[1]. Chemical drugs have been used for the elimination of *P. falciparum*, such as artemisinin and its derivatives[2−5]. As a good antimalarial drug, chloroquine soon lost its therapeutic effect on *P. falciparum* after the emergence of resistant strains[6−8]. Chloroquine has been removed from first-line antimalarial for the elimination of *P. falciparum* by World Health Organization (WHO). In areas with chloroquine-susceptible infections, chloroquine is indicated for the treatment of uncomplicated *Plasmodium vivax*, *Plasmodium ovale*, *Plasmodium malariae* or *Plasmodium knowlesi* malaria[9]. A large number of studies have shown that chloroquine resistance is strongly associated with mutations of the *Pfcrt* gene, which encodes the chloroquine resistance transporter to participate in efflux chloroquine from the intracellular digestive vacuole, the site of drug action[10,11]. *Pfmdr1* gene mutation is also related to the production of chloroquine resistance[12−14]. Artemisinin-based combination therapy has become the standard antimalarial therapy recommended by the WHO, and is considered to be the most effective treatment for severe malaria[15]. It is disappointing that the emergence of artemisinin-resistant strains is a serious challenge for artemisinin-based combination therapy[16,17]. New antimalarial drugs are urgently needed for malaria elimination campaigns. Targeted biological drugs are becoming a new direction of malaria drug research and development. Antigens expressed on the surface of merozoites are considered blood stage malarial vaccine candidates, some of which are in clinical testing, *e.g.*, reticulocyte-binding protein homolog 5 (RH5), part of a trophozoite-exported protein (P27A), merozoite surface protein 3, and apical membrane antigen 1[18]. Zhang et al.[19] previously identified a new pair of ligand−receptor proteins, *i.e.*, rhoptry-associated protein 2 (RAP2), a rhoptry protein expressed on the surface of merozoites, and its receptor CD147 on erythrocytes. Their interaction occurs in the parasitophorous vacuole formation stage of the invasion. Zhang et al.[19] demonstrated that HP6H8 also known as meplazumab, a humanized CD147 monoclonal antibody (mAb), exhibited excellent efficacy in the treatment and prevention of severe malaria in humanized mice, and it is believed that it would become a novel targeted antimalarial drug in the blood stage.

Compared with traditional chemical drugs, monoclonal antibodies have obvious advantages, including high specificity, low toxicity, long half-life in the blood, etc. In the treatment of diseases, both the variable region (Fab) and crystalline region (Fc) of mAbs can play an important role. The Fab segment of mAbs can perform its biological function by identifying free targets in the blood circulation or by targeting proteins on the cell surface[20,21]. The Fc segment of mAbs can enhance the immune defense mechanism by antibody-dependent cell-mediated cytotoxicity (ADCC), antibody-dependent cytophagy, and complement dependent cytotoxicity effects[22−24]. Zhang et al.[19] have demonstrated that the Fab segment of meplazumab blocked the invasion of *P. falciparum* by targeting CD147 on the erythrocyte surface.

Detailed preclinical pharmacokinetic and toxicology data of mAbs determine whether they can be used in human clinical trials[25]. The pharmacokinetic study of mAbs can provide us with data on the tissue distribution, metabolic pathway, and retention time *in vivo*. Traditional non-antibody drugs have a half-life of only a few hours, while mAbs have a serum/plasma half-life of several days or more in humans. Parenteral administration, slow tissue distribution, and a long elimination half-life are the most pronounced clinical pharmacokinetic characteristics of mAbs. Monoclonal antibodies have gained distinct competitive advantages in the field of biopharmaceuticals. However, several mAbs have been discontinued or withdrawn based either on their inability to demonstrate efficacy and/or due to adverse effects, *e.g.*, efalizumab[26]. Furthermore, even some of the mainstream anti-cancer mAb drugs have had some adverse events reported. These adverse events have mainly manifested as toxic and side effects to different organ systems during the administration of mAbs, including anemia, allergic reactions, gastrointestinal toxicity, neurotoxicity, cardiotoxicity, etc.[27−29]. The association between these adverse events and the mAbs remains to be confirmed, but it still demonstrates the importance of preclinical toxicology studies. Preclinical toxicology studies of mAbs allow people to predict and handle the potential side effects and clinical toxicity in humans. Suitable animal models are very important for the study of preclinical pharmacokinetics and toxicology of mAbs[30]. Animal models should have similar pharmacology, pharmacokinetic and toxicology profiles to humans[31−33]. At present, Sprague−Dawley (SD) rats, pigs, dogs, and non-human primates are widely used in preclinical studies of mAbs. More nonclinical safety and tolerance evaluations of meplazumab are needed to support its clinical trials.

CD147 is a highly glycosylated type 1 single transmembrane glycoprotein, belonging to the immunoglobulin superfamily. CD147 is an important adhesion molecule and plays a significant role in numerous pathological processes, including cancer, inflammation, atherosclerosis, and ischemic myocardial injury[34]. CD147 is expressed on erythrocyte lineage cells throughout erythroid development, including mature erythrocytes, and is the target for *Plasmodium* merozoites to allow reorientation and subsequent invasion of erythrocytes. Specifically, CD147 interacts with RH5 to facilitate the relocation of *P. falciparum* on the surface of erythrocytes[35,36] and with the parasite ligand RAP2 to

promote the formation of the *P. falciparum* parasitophorous vacuole[19]. As meplazumab binds to CD147 expressed on the human erythrocyte cell surface through the complementary determining region, it directly blocks the CD147−RAP2 interaction and the formation of the parasitophorous vacuoles needed for *P. falciparum* invasion of human erythrocytes. This is a different mechanism from other anti-falciparum malaria drugs. Zhang et al.[19] found that the CD147−RAP2 interaction is essential for *P. falciparum* to invade human erythrocytes and confirmed that the anti-CD147 mAb meplazumab can effectively treat and prevent *P. falciparum* invasion of human erythrocytes *in vitro* and *in vivo*. The efficacy against chloroquine-resistant *P. falciparum* of meplazumab *in vivo* is still unclear.

In this study, we demonstrated that meplazumab was safe and tolerated in cynomolgus monkeys and SD rats. In addition, within the given concentration range, meplazumab had a low cross-reactivity rate in various tissues and did not cause hemolysis or aggregation of red blood cells (RBCs). Finally, we evaluated the efficacy against chloroquine-resistant *P. falciparum* of meplazumab in a humanized mouse model. Taken together, the nonclinical data provided by this study are an important basis for the clinical research and application of meplazumab.

2. Materials and methods

2.1. Cell lines and cell culture

The human lung cancer cell line A549 was obtained from American Type Culture Collection (Manassas, VA, USA). After expansion, this cell line was deposited into the National Platform of Experimental Cell Resources for Sci-Tech (Beijing, China). This cell line was subjected to short tandem repeat tests and authenticated before utilization for researches. This cell line was maintained in high-glucose DMEM supplemented with 10% fetal calf serum at 37 °C and 5% CO_2 in a humidified incubator.

2.2. Meplazumab

Meplazumab is a recombinant, humanization IgG2 antibody constructed by complementary determining region-grafting, directed against the extracellular region of human CD147. Meplazumab is produced by cell culture in bioreactors, using serum-free media at Pacific Meinuoke Biopharmaceutical Co., Ltd. (Changzhou, China). After purification, the mAb was resolved in histidine/histidine hydrochloride buffer solution (pH 7.2) containing polysorbate 80 and sucrose, vialed under aseptic conditions, and formulated as a colorless, sterile product without any preservatives.

2.3. Reagents

Metuzumab was supplied by Pacific Meinuoke Biopharmaceutical Co., Ltd. RPMI medium 1640 (72,400-047) was purchased from Gibco (Grand Island, NY, USA). Hypoxanthine (H9377-5G) and chloroquine (C6628-25G) were purchased from Sigma−Aldrich (St. Louis, MO, USA). Clodronate liposomes were purchased from Liposoma B.V. (Amsterdam, The Netherlands). IgG from human serum was purchased from Genia (Beijing, China). Anti-human CD235a PE antibody (12-9987-82, RRID: AB_466,300) was purchased from Thermo-Fisher (Waltham, MA, USA). CD147-his protein and anti-meplazumab polyclone antibody were supplied by Fourth Military Medical University (Xi'an, China). Human IgG-heavy and light chain monkey-adsorbed antibody conjugate horseradish peroxidase (HRP) was purchased from Bethyl (Montgomery, AL, USA). ^{125}I-Meplazumab was supplied by MITRO Biotech Co., Ltd. (Nanjing, China). The CD31 antibody (11265-1-AP) was purchased from Proteintech Group, Inc. (Wuhan, China).

2.4. Animals

NOG (NOD/Shi-scid/IL-2Rγ null, female, 12 weeks old) mice were purchased from Beijing Vital River Laboratory Animal Technology Co., Ltd. (Beijing, China). All experiments were performed under specific-pathogen-free conditions and obeyed the experimental animal protocols that were approved by the Laboratory Animal Welfare and Ethics Committee of Medical Department of Fourth Military Medical University (Xi'an, China).

SD rats (half of each sex, 180−220 g) were purchased from Beijing Vital River Laboratory Animal Technology Co., Ltd. SD rats were received according to the standard operating procedures of MITRO Biotech Co., Ltd. (Nanjing, China), and the experimental animals were housed in the barrier facility for specific-pathogen-free animals. Experimental animal use permission was SYXK (Su) 2015−0014.

Cynomolgus monkeys (half of each sex, 2.8−4.7 kg) for toxicology studies were provided by Guangdong Chunsheng Biological Technology Development Co., Ltd. (Guangzhou, China). The cynomolgus monkeys were chosen as the non-rodent species for drug safety evaluation because it is accepted by health authorities worldwide as an appropriate experiential animal model. Meanwhile, since the test article is a humanized monoclonal antibody, cynomolgus monkeys are very sensitive to it. The toxicology studies were conducted in compliance with the "Guide for the Care and Use of Laboratory Animals" (2011) issued by the National Research Council, USA, and the "Laboratory Animal Administration" (2nd edition, 1988) issued by the State Science and Technology Committee, China.

2.5. Surface plasmon resonance measurements

The affinity (K_D) for the binding of human and cynomolgus monkey CD147 antigens to meplazumab was measured on a multi-SPR array system (ProteOn XPR36, Bio-Rad, Hercules, CA, USA). Briefly, meplazumab (10 μg/mL) was fixed to the chip, and various concentrations of CD147 extracellular protein from humans and cynomolgus monkeys (0, 0.625, 1.25, 2.5, 5 and 10 nmol/L) were injected into different channels. After 3 min of binding and 12 min of dissociation at a flow rate of 50 μL/min, the obtained data were analyzed using the Langmuir model (1:1).

2.6. Flow cytometry assay

Levels of CD147 expression on erythrocytes from different species were evaluated using flow cytometry. RBCs from humans (7 cases) and cynomolgus monkeys (10 cases) were incubated with meplazumab (4 or 40 μg/mL) at 37 °C for 1 h. An anti-human IgG antibody was incubated at 4 °C for 1 h. After rinsing twice, the results were detected using flow cytometry.

2.7. A 4-week repeat-dose intravenous toxicology study of meplazumab in cynomolgus monkeys with an 8-week recovery period

A total of 40 cynomolgus monkeys were assigned into four groups: vehicle control group (solvent of meplazumab for injection: 0 mg/kg/day), and meplazumab groups at low (2 mg/kg/day), middle (6 mg/kg/day), and high (12 mg/kg/day) doses. The dose volume was 5 mL/kg. Each group consisted of 10 animals (half of each sex). Animals were dosed once weekly (Days 1, 8, 15 and 22, respectively). Necropsy was performed in 6 animals (half of each sex) at the end of the dosing period and the remaining 4 animals (half of each sex) at the end of the recovery period. Tissues/organs were collected and processed for histopathological examination. The toxicological endpoints evaluated during the dosing and recovery periods included the following: mortality/moribundity observations, clinical observations, dose site irritation observation, body weight, food consumption, rectal temperature, electrocardiogram (lead II), blood pressure, respiratory rate, ophthalmology examination, hematology/coagulation/clinical chemistry/immune function, urinalysis, occult blood analysis in feces, and bone marrow smear examination.

Blood samples were drawn from the femoral veins on the opposite side of the injection sites at different time points from all animals for toxicokinetic analysis. For the vehicle group, blood samples were collected pre-dosing and 4 h post dosing. For meplazumab groups, during the first dosing, blood samples were collected pre-dosing and at 0.25, 4, 24, 48, 72, 96 and 168 h (pre-dosing on Day 8) post-dosing; during the fourth dosing, blood samples were collected pre-dosing and at 0.25, 4, 24, 48, 72, 96, and 168 h post-dosing. All blood samples were collected into the tubes containing separation gel and coagulant, and kept on crushed ice. The collected blood samples were centrifuged at approximately 3500 rpm (Beckman, Brea, CA, USA) for 5 min at 4 °C. After centrifugation, the serum samples were separated and stored at −80 °C until further analysis.

Serum concentration of meplazumab will be determined using a validated ELISA method. Briefly, for the quantification of meplazumab in serum samples, 96-well-microplates were coated with CD147-his coating solution. Meplazumab in the samples were combined with antibody-coated plate, then human IgG-heavy and light chain monkey-adsorbed antibody conjugate HRP was added. Responses were developed using tetramethylbenzidine as substrate, and the reaction was stopped with H_2SO_4 solution. The absorbance at 450 nm/630 nm was then read by Microplate Reader (Epoch, BioTek Instruments, Inc., Winooski, VT, USA). Toxicokinetic parameters, including (if applicable) but not limited to C_{max}, T_{max}, and $AUC_{0-168\ h}$, were calculated using Watson 7.4 software (Thermo-Fisher).

2.8. Anti-drug antibody (ADA) assays

In toxicology study, all surviving animals were submitted for immunogenicity test. Serum samples were collected for the immunogenicity analysis at acclimation period (once), Days 14 and 28 (dosing period), 42, 56, 70, and 84 (recovery period).

ADA in cynomolgus monkey serum following injection of meplazumab was detected using validated bridging ELISA methods. Briefly, microplates were coated with meplazumab, incubated at 2−8 °C overnight, and then blocked with 5% skimmed milk powder for at least 2 h. Samples were diluted 20 times with 1% albumin from bovine serum and added to each well. Biotin-labeled meplazumab was then added. The "test item-ADA–test item" complex formed was detected with the streptavidin-HRP in combination with tetramethylbenzidine substrate. The chromogenic reaction was stopped with stop solution, and the signal at 450 nm/560 nm was recorded by Microplate Reader (Epoch, BioTek Instruments, Inc.). The intensity of the signal was positively correlated with the concentration of the ADA for meplazumab.

2.9. In vitro hemolysis studies

New Zealand white rabbits are internationally accepted non-rodent species for assessment of the hemolysis test of pharmaceuticals. One New Zealand white rabbit (female, 3.2 kg) was purchased from Chinese Food and Drug Inspection Institute (Beijing, China) and housed in the barrier facility for specific-pathogen-free animals. Experimental animals use license number is SYXK (Hu) 2014-0009. Cynomolgus monkeys were chosen to evaluate the safety of meplazumab *in vivo* in this study. Therefore, in *in vitro* hemolysis studies, the blood from New Zealand white rabbit and cynomolgus monkey were used to assess the potential hemolysis test. In addition, the maximal intended clinical concentration of meplazumab was 2 mg/mL. The operation was as follows. The whole blood collected from a New Zealand white rabbit and a cynomolgus monkey was gently shaken for 10 min using flash with beadings for removing fibrin. RBCs were isolated after centrifugation (Beckman, 1500 rpm for 15 min) using an appropriate amount of 0.9% sodium chloride injection at room temperature. The above procedures were repeated 2 times until transparent and colorless supernatants were obtained. A 2% RBC suspension was prepared by diluting with 0.9% sodium chloride injection. The groups were divided into negative control (0.9% sodium chloride injection), vehicle control, positive control (deionized water), and meplazumab (different concentrations, the max concentration up to 2 mg/mL) groups. The RBCs of New Zealand white rabbit and cynomolgus monkey were mixed with test article or control. The character of solution was observed at 15, 30, 45, 60, 120 and 180 min after incubation at 37 °C. The solution showed red transparent indicating hemolysis. Brown-yellow or red-brown floccule deposition was observed in solution when RBCs aggregated and the solution did not disperse after vibration.

2.10. Tissue cross-reactivity studies

A tissue cross-reactivity study was performed on normal tissues from humans and cynomolgus monkeys by immunohistochemical staining. The normal human tissues were collected from the department of pathology, Xijing hospital (Xi'an, China). All individuals provided written informed consent, and the study was approved by the Hospital Ethics Committee (Xi'an, China).

In order to detect the binding ability, the test article was applied to formalin-fixed paraffin-embedded (FFPE) slices of normal human, and cynomolgus monkey tissues (3−8 donors per tissue) at two concentrations. Meplazumab at 1 μg/mL was selected as the low concentration, and meplazumab at 20 μg/mL was selected as the high concentration. The blank control was 1 × phosphate buffered saline (PBS), and an anti-CD31 antibody directed against CD31, an endothelial cell biomarker, was used as an antigen preservation system control. Human lung adenosquamous carcinoma and hepatocellular carcinoma tissues were selected as the positive control tissues.

The FFPE slices were deparaffined and dehydrated following standard protocols. The antigens were retrieved by autoclaving in citric acid buffer (pH 6.0). Endogenous peroxidase was quenched by peroxidase blocking solution, and endogenous biotin was blocked by nonspecific staining blocker. After rinsing, the FFPE slices were incubated with meplazumab (1 or 20 μg/mL), rabbit anti-human/monkey CD31 polyclonal antibody or PBS, at 4 °C overnight. After washing with PBS, the FFPE slices were incubated with biotinylated-coupled secondary antibodies according to the type of primary antibody for 15 min at room temperature. After incubation with peroxidase-labeled streptavidin, the FFPE slices were developed in 3,3-diaminobenzidine and counterstained with hematoxylin. The FFPE slices were dehydrated, mounted, and visualized under a light microscope. The expression level was evaluated by two senior pathologists.

2.11. *Distribution and excretion in SD rats*

Meplazumab was labeled with ^{125}I through the iodogen method. The stability of the ^{125}I-meplazumab labeled material was confirmed before injection. Trichloroacetic acid (TCA) precipitation was used to validate the methodology of ^{125}I-meplazumab for the tissue distribution study.

Twenty-four SD rats (half of each sex) were administrated ^{125}I-meplazumab at about 1 mg/kg or 20 ± 10 μCi per animal by a single intravenous injection. A group of 6 animals were sacrificed at 2, 96, 168, and 240 h post-administration. The urine, whole blood (preparation for whole blood, plasma, and hemocytes), heart, liver, spleen, lungs, kidneys, stomach, intestine, gonads, brain, fat, skeletal muscles, femurs, adrenal gland, thymus, mesenteric lymph nodes, and thyroid tissues were collected. The total radioactivity of the samples, as well as those after TCA precipitation, was measured using a gamma meter (Biodex, New York, NY, USA). Plasma and urine samples were collected from 1 female rat and 1 male rat at 2, 96, 168, and 240 h, and separated by high-performance liquid chromatography (HPLC, Biodex). The elution was measured using a gamma meter (Biodex), and diagrams were drawn using radioactivity *versus* time.

Six bile duct intubation model SD rats were administrated with ^{125}I-meplazumab at approximately 1 mg/kg or 20 ± 10 μCi per animal by a single intravenous injection. Bile fluids were collected at 0−4, 4−8, 8−24, and 24−48 h post-administration. The total radioactivity of each sample was measured using a gamma meter (Biodex), and the cumulative recovery of radiolabeled samples excreted through the bile fluid path at each time point was calculated.

Six normal SD rats were administrated ^{125}I-meplazumab at approximately 1 mg/kg or 20 ± 10 μCi per animal by a single intravenous injection. Urine and feces were collected at 0−8, 8−24, 24−48, 48−96, 96−168, 168−336, 336−504, 504−672, 672−840, 840−1008, and 1008−1176 h post-administration. The total radioactivity of each sample was measured using a gamma meter (Biodex). The cumulative percentage of radiolabeled samples excreted through the urine and feces paths at each time point were calculated.

2.12. *ADCC assays*

In vitro ADCC assays were performed as previously described[37]. Briefly, the ADCC assays of meplazumab were performed using human peripheral blood mononuclear cells isolated from the blood of healthy humans (n = 2) as the effector cells, and the non-small-cell lung cancer A549 cells overexpressing CD147 as target cells. The target cells (1×10^4 per well) were pre-incubated with different concentrations (12.5, 25, 50, 100, 200, 400, 600, 800, and 1000 μg/mL) of meplazumab or control antibody (metuzumab) for 30 min, prior to the addition of the effector cells at an effector/target ratio of 50:1. The cells were incubated for an additional 4 h and then the cell death was detected by measuring lactate dehydrogenase activity using a Cytotoxicity Detection Kit (Roche, Basel, Switzerland) according to the manufacturer's protocols as in Eq. (1):

$$\text{Cytotoxicity (\%)} = (\text{Experimental cell lysis} - \text{Spontaneous effector lysis} - \text{Spontaneous target lysis})/(\text{Maximum target lysis} - \text{Spontaneous target lysis}) \times 100 \quad (1)$$

All samples were assayed in triplicate wells in two independent experiments. The calculation of concentration for 50% of maximal effect was based on the four-parameter fitting curve.

2.13. *Antimalarial efficacy of meplazumab in humanized mice*

The establishment of a humanized mouse model infected with chloroquine-resistant strain referred to previous construction methods[19]. Briefly, NOG mice were injected with 450 μL of type O human red blood cells (huRBCs), 250 μL of human serum from a type AB donor mixture *via* the inner canthus veniplex and 500 μL of a 20% clodronate liposomes mixture (100 μL of clodronate liposomes + 400 μL of RPMI 1640 + 50 mg/L hypoxanthine) by intraperitoneal injection three times a week. Subsequently, peripheral blood cells were collected *via* tail vein and incubated with anti-human CD235a PE (1:1200) for 40 min at room temperature. Samples were rinsed with PBS. The chimerism rate of the huRBCs was determined by flow cytometry (LSRFortessa™, BD Pharmingen, San Diego, CA, USA). Mice with chimerism rate of more than 30% were randomized into groups. The mouse models were divided into negative control (IgG from human serum, 5 mg/kg), positive control (chloroquine, 5 mg/kg), and meplazumab (5 mg/kg) groups. The cultured *P. falciparum* Dd2, which had not been synchronized, was used for infection when the parasite rate reached 1%. One hundred microliters of pure RBCs with a 1% parasite rate was mixed with 250 μL of human type AB serum. The mixture was injected *via* the inner canthus veniplex of mouse.

After infection, peripheral blood was sampled *via* the inner canthus veniplex of the mice to prepare a thin blood smear every day. After Giemsa staining, the number of parasite-infected RBCs among a total of 10,000 RBCs was counted microscopically for calculation of parasitemia (Pr) as Eq. (2):

$$\text{Pr (\%)} = \text{Number of RBCs infected with parasites}/10{,}000 \times 100 \quad (2)$$

The inhibition rate (IR) at each time point and dosing group was calculated by Eq. (3):

$$\text{IR}_{\text{treatment}}\ (\%) = (1 - \text{Pr}_{\text{treatment}}/\text{Pr}_{\text{negative}}) \times 100 \quad (3)$$

The clearance rate refers to the percent of mice with complete elimination of *P. falciparum* (Pr = 0) in their RBCs accounting for the total number of mice in each group, and the median

parasite clearance time (PC_{50}) of mice in each group was estimated.

2.14. Receptor occupancy (RO) assays

The RO rate on erythrocytes after *in vitro* incubation of meplazumab with human peripheral blood was measured using flow cytometry. Peripheral venous blood was collected from four volunteers, and a series of different concentrations of meplazumab was spiked in for *in vitro* incubation. The drug on the blood cell surface was then detected using a biotin labeled anti-human IgG antibody. Erythrocytes were gated using CD235a which is an RBC surface marker, and the RO rate was then calculated. The drug concentrations and RO rates were fitted to obtain a drug concentration−receptor occupancy level curve. This curve was then used to calculate the concentration of meplazumab added at a RO of 10%, 20%, 50%, and 90%.

2.15. Statistical analysis

The statistics of P and IR in antimalarial activity study of meplazumab are presented as the mean ± SEM. The statistics of exposure of the analytes (AUC and C_{max}) were performed after being converted to logarithm scale. The same parameters in comparison between two groups used a *t* test, and the relationship between drug exposure and dose was statistically analyzed using SPSS Statistics 21 (IBM, Armonk, NY, USA).

3. Results

3.1. Meplazumab exhibits high affinity with CD147 from humans and cynomolgus monkeys

To select relevant species for toxicology studies, the affinity of meplazumab with CD147 from different species was evaluated.

As shown in Fig. 1A and B, the affinity constants (K_D values) in humans, and cynomolgus monkeys were determined to be 1.51×10^{-10} and 1.26×10^{-9} mol/L, respectively. Meplazumab was confirmed to bind to CD147 humans and cynomolgus monkeys. The K_D value of human CD147 was higher than that in cynomolgus monkeys.

Furthermore, meplazumab binding to CD147 expressed on erythrocytes from different species was also evaluated using flow cytometry. Meplazumab was able to bind erythrocytes of humans and cynomolgus monkeys. Meplazumab exhibited higher level of binding with erythrocytes of humans than that with erythrocytes of cynomolgus monkeys (Fig. 1C and Supporting Information Table S1).

Taken together, these results indicated that meplazumab exhibited binding activity to CD147 from humans and cynomolgus monkeys. The affinity in humans is 13.5-fold higher than that in cynomolgus monkeys. Compared with the amino acid sequences of CD147 in *homo sapiens*, the homology of CD147 in cynomolgus monkeys is 85%. The binding of meplazumab with the RBCs of cynomolgus monkeys also indicated that this species is appropriate for toxicology evaluation of meplazumab.

3.2. ADCC activity of meplazumab

The life cycle of *P. falciparum* in erythrocytic stage occurs in human erythrocytes. Previous studies have demonstrated the treatment of various diseases depends on ADCC activity of antibody[37−39].

To evaluate ADCC activity of meplazumab on human cells, an ADCC assay *in vitro* was conducted in this study. As shown in Fig. 1D and Supporting Information Table S2, meplazumab showed weak cytotoxicity (<7.51%) to A549 cells overexpressing CD147, but no clear concentration-dependent relationship was found among the groups and the concentration for 50% of maximal effect could not be calculated. Meplazumab could not induce ADCC activity at concentrations up to 1 mg/mL. In contrast, metuzumab, the positive control, showed significant cytotoxicity among the dose groups. We inferred that meplazumab had no ADCC effect on human erythrocytes.

3.3. Hemolysis studies in New Zealand white rabbits and cynomolgus monkeys

To further evaluate the effect of meplazumab on erythrocytes, hemolysis studies *in vitro* were conducted. The whole blood cells were collected from New Zealand white rabbits and cynomolgus monkeys. As shown in Supporting Information Tables S3 and S4, no hemolysis and RBC aggregation were observed for the test article, negative control or vehicle control at 15, 30, 45, 60, 120 and 180 min after incubation. The positive control tube was red and transparent at the above time points. Above all, meplazumab at 2 mg/mL did not cause hemolysis or aggregation of RBCs isolated from New Zealand white rabbits and cynomolgus monkeys.

3.4. Repeat-dose toxicity profiles of meplazumab in cynomolgus monkeys

In the repeat-dose toxicology study, one female animal in the 12 mg/kg group died on Day 22 due to excessive anesthesia. All other animals survived until the scheduled necropsy. No meplazumab-related changes were observed in clinical observations, body weight, food consumption, rectal temperature, ophthalmology, coagulation, clinical chemistry, immune function, bone marrow smear, urinalysis, or occult blood in feces examination in all animals during the whole study (Supporting Information Figs. S1 and S2, and Tables S5–S13).

For clinical hematology, compared with the 0 mg/kg group, increased percentage reticulocyte count was observed in males and females in the 6 and 12 mg/kg groups at the end of the dosing period (Supporting Information Tables S7 and S8). These changes were completely reversed at the end of the recovery period.

For clinical chemistry, as shown in Supporting Information Tables S9 and S10, in the 2 mg/kg group, no significant changes were observed in either males or females in comparison with the 0 mg/kg group. However, increased alanine aminotransferase in 1 of 5 females were observed on Day 28, as compared with the base values prior to administration. In the 6 mg/kg group, no significant changes were observed in either males or females in comparison with the 0 mg/kg group. However, increased alanine aminotransferase in 1 of 5 females and increased total bile acid in 1 of 5 females were observed on Day 28, as compared with the base values prior to administration.

As compared to the 0 mg/kg group, sporadic and dose-independent significant changes were considered unrelated to meplazumab and toxicologically insignificant. There were no meplazumab-related macroscopic or microscopic findings noted at

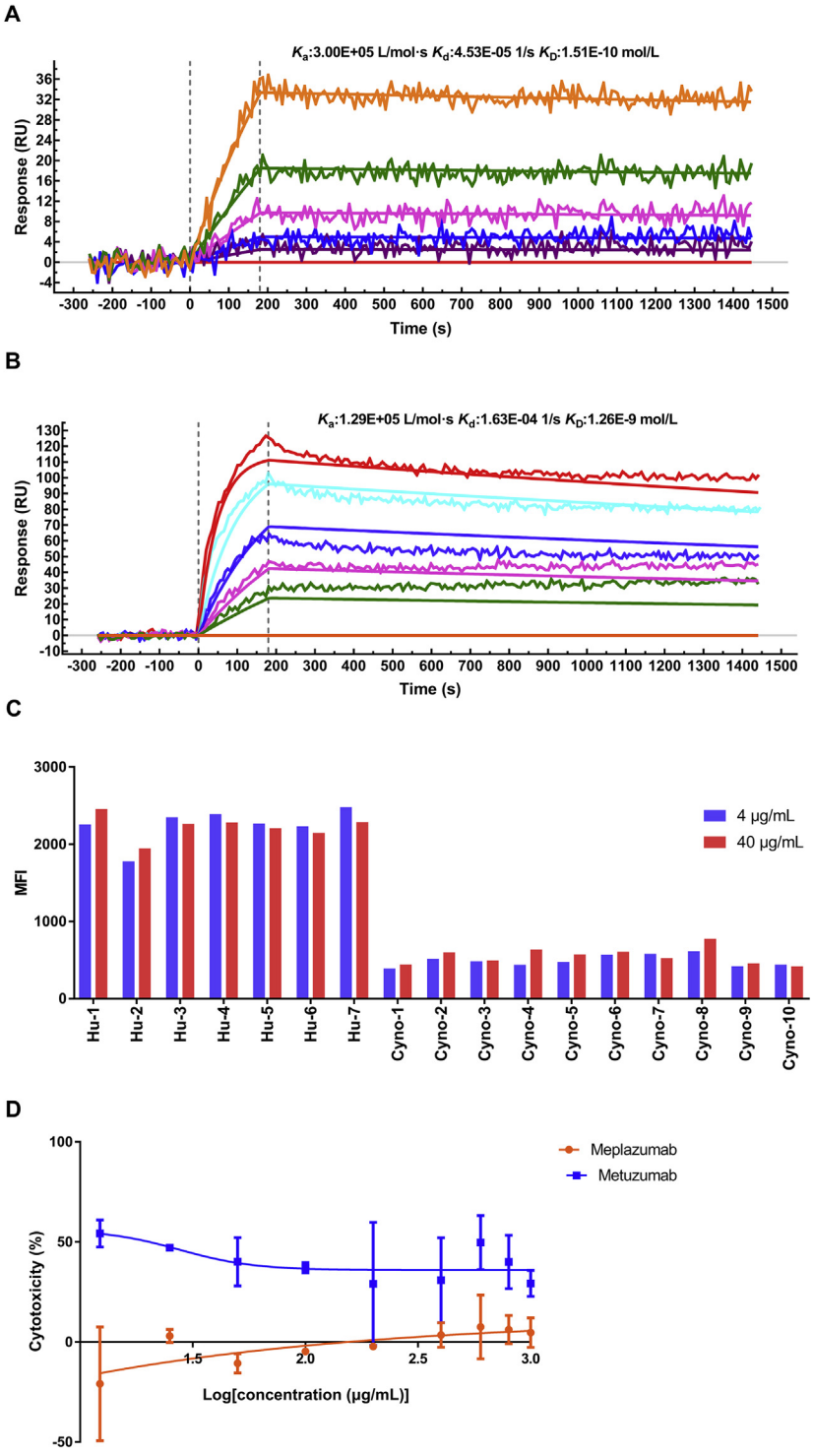

Figure 1 *In vitro* characterization of meplazumab. The kinetic analysis of meplazumab binding to (A) human, and (B) cynomolgus monkey CD147 was performed by surface plasmon resonance measurements using a ProteOn XPR 36. (C) Meplazumab binding to red blood cells from different species was detected by flow cytometry. Meplazumab affinity was determined using median fluorescence intensity (MFI). (D) ADCC activity of meplazumab *in vitro*. The cytotoxicity of meplazumab and metuzumab on human peripheral blood mononuclear cells was measured using lactate dehydrogenase release assay. A549 cells expressing CD147 were used as target cells. Hu, human; Cyno, cynomolgus monkey.

any of the dose levels. Under the experimental conditions of this study, the major changes of meplazumab on cynomolgus monkeys included increased percentage reticulocyte count dosed at >6 mg/kg, considered to be a pharmacodynamics effect. The above alterations were reversible. Under the conditions of this study, no observed adverse effect level was considered to be at 12 mg/kg with corresponding $AUC_{0-168\ h}$ of 19,123 μg·h/mL in males and 11,830 μg·h/mL in females.

3.5. *Repeat-dose toxicokinetics studies of meplazumab in cynomolgus monkeys*

The *in vivo* repeated-dose toxicokinetics study in cynomolgus monkeys was performed together with repeated-dose toxicity study in cynomolgus monkeys. The results are shown in Fig. 2A−D and Table 1. For the animals dosed with meplazumab in the range of 2−12 mg/kg, the serum concentration of meplazumab increased with the dose level during the first and fourth dosing. There was no statistical difference of $AUC_{0-168\ h}$ and C_{max} between male and female animals during the first and fourth dosing in each group. As the dose increased from 2 to 12 mg/kg, the C_{max} increased in a greater than dose-dependent manner. For the animals dosed with the meplazumab in the range of 2−12 mg/kg, C_{max} and $AUC_{0-168\ h}$ did not have a proportionality with dose levels during the first and fourth dosing.

As shown in Table 1, after 4 weeks of repeated intravenous administration, no significant increase in exposure ($AUC_{0-168\ h}$) or accumulation of drug exposure was observed in low-, medium- and high-dose groups of meplazumab, and no accumulated exposure was observed in both females and males. The $AUC_{0-168\ h}$ ratio (fourth dosing *versus* first dosing) in female

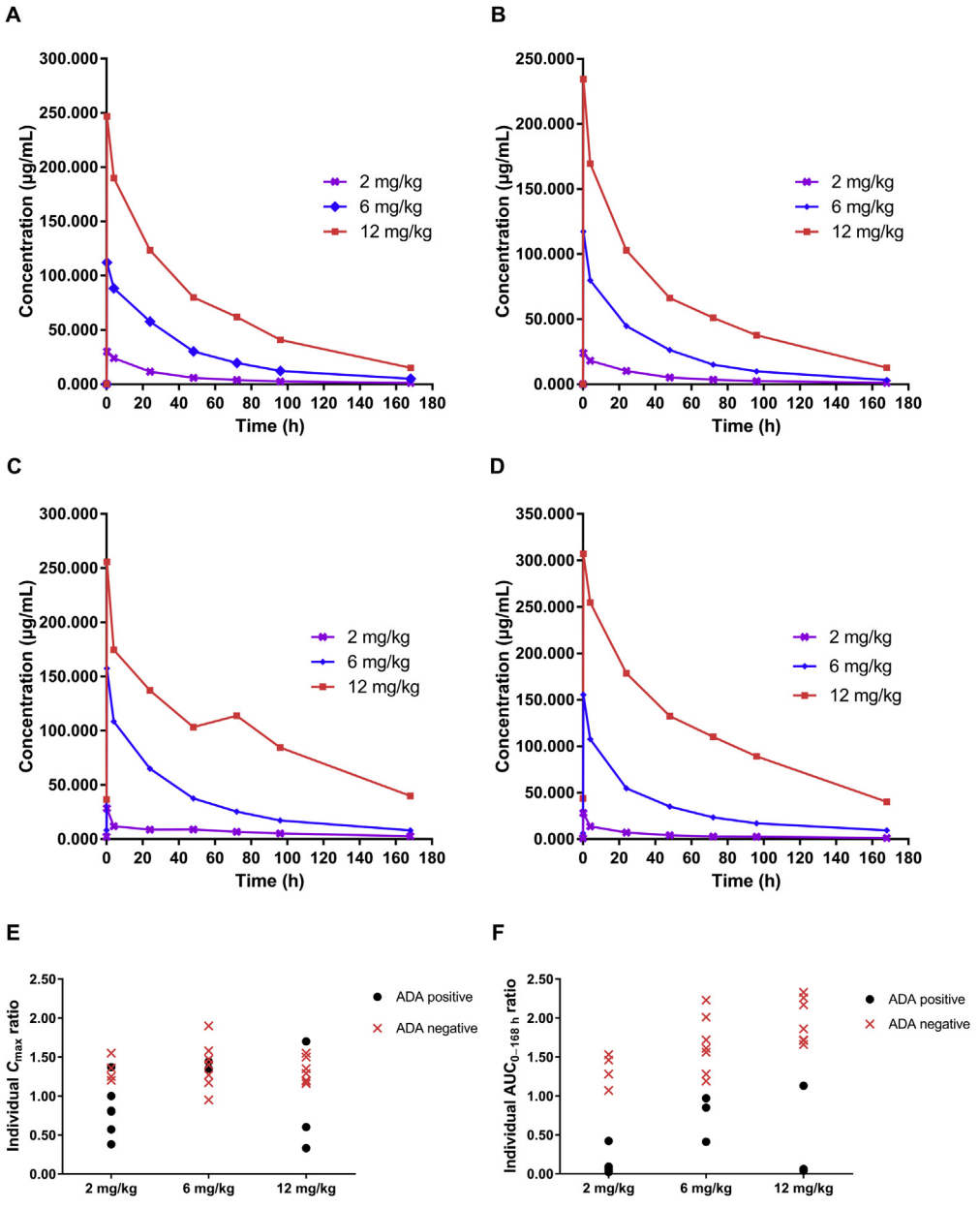

Figure 2 Serum concentration profiles of meplazumab in the cynomolgus monkeys. The mean serum concentration−time course of meplazumab after the first intravenous dose in (A) female animals and (B) male animals. The mean serum concentration−time course of meplazumab after the fourth intravenous dose in (C) female animals and (D) male animals. (E) The ratio of the individual C_{max} of the fourth to first injection of meplazumab in ADA-positive and ADA-negative cynomolgus monkeys in the different repeat-dose groups during the dosing period. (F) The ratio of individual $AUC_{0-168\ h}$ of the fourth to first injection of meplazumab in ADA-positive and ADA-negative cynomolgus monkeys in the different repeat-dose groups during the dosing period.

Table 1 Toxicokinetic parameters of meplazumab in cynomolgus monkeys in repeat-dose toxicity study.

Group	Gender	Sample	C_{max} (μg/mL)	$AUC_{0-168\ h}$ (μg·h/mL)	T_{max} (h)		
					Median	Min	Max
2 mg/kg	Male	Day 1	25 ± 9	853 ± 156	0.25	0.25	24.00
		Day 22	28 ± 11	508 ± 509	0.25	0.25	0.25
	Female	Day 1	30 ± 4	1010 ± 71	0.25	0.25	4.00
		Day 22	28 ± 18	640 ± 808	0.25	0.25	0.25
6 mg/kg	Male	Day 1	117 ± 5	3755 ± 607	0.25	0.25	0.25
		Day 22	155 ± 29	5287 ± 2092	0.25	0.25	0.25
	Female	Day 1	112 ± 30	4513 ± 843	0.25	0.25	0.25
		Day 22	158 ± 22	5551 ± 1208	0.25	0.25	0.25
12 mg/kg	Male	Day 1	234 ± 22	9821 ± 1475	0.25	0.25	0.25
		Day 22	307 ± 32	19,123 ± 2726	0.25	0.25	0.25
	Female	Day 1	247 ± 20	11,375 ± 1403	0.25	0.25	0.25
		Day 22	256 ± 136	11,830 ± 10,649	0.25	0.25	0.25

Day 1, first dosing; Day 22, fourth dosing; the C_{max} and AUC results represent the mean ± SEM.

animals were 0.60, 1.27 and 1.02, respectively in low-, medium- and high-dose groups of meplazumab. The $AUC_{0-168\ h}$ ratio (fourth dosing *versus* first dosing) in male animals were 0.61, 1.50 and 1.97 respectively in low-, medium- and high-dose groups of meplazumab.

3.6. *Effect of ADA on drug exposure in cynomolgus monkeys*

The immunogenicity study was performed together with the repeated-dose toxicity study in cynomolgus monkeys. ADA was detected in 8/10 animals in 2 mg/kg group, 6/10 animals in 6 mg/kg group and 4/10 animals in 12 mg/kg group at the end of the recovery period (Table 2). Among the 187 tested samples, 58 were confirmed as positive, making the positive rate of 31.02%. The results of screening and confirmation tests indicated that positive animals were detected in all groups. ADA was detected more frequently in the 2 mg/kg group than in higher dose groups.

In 6 mg/kg group, the ratios of C_{max} of the fourth to first injection of meplazumab in ADA positive animals were similar to that in ADA negative animals, while in 2 mg/kg group and 12 mg/kg group, higher variability of the ratios of C_{max} was exhibited between ADA positive animals and ADA negative animals (Fig. 2E). The ratio of $AUC_{0-168\ h}$ of the fourth to first injection of meplazumab in ADA positive animals were lower than that in ADA negative animals (Fig. 2F). As shown in Table 3, The $AUC_{0-168\ h}$ of ADA positive animals in low, medium and high dose levels, respectively, lower than that of ADA negative animals in low, medium and high dose levels, respectively. The variability of C_{max} and $AUC_{0-168\ h}$ in ADA positive animals was higher than that in ADA negative animals. It is indicated that the presence of ADA in ADA-positive animals was associated with accelerated drug clearance.

Table 2 Immunogenicity detection results in cynomolgus monkeys in repeat-dose toxicity study.

Dosing (mg/kg)	Number of animals (M/F)	Number of positive animals	Proportion of positive animals (%)
0	5/5	0	0
2	5/5	8	80
6	5/5	6	60
12	5/5	4	40

M, male; F, female. The results were collected from the immunogenicity detection of all surviving animals before necropsy during the dosing and recovery periods.

3.7. *Tissue cross-reactivity study*

To further evaluate the safety of meplazumab, a tissue cross-reactivity study was evaluated in FFPE slices from 32 kinds of normal human tissues and 33 kinds from normal tissues of cynomolgus monkeys by immunohistochemical staining.

The detection results of FFPE slices are shown in Supporting Information Table S14. Tissue cross-reactivity studies in different species showed similar staining patterns in the vast majority of the tissue samples from humans and cynomolgus monkeys. Negative staining with meplazumab at the low concentration (1 μg/mL) was observed in all kinds of normal human and cynomolgus monkey tissues. At the high concentration (20 μg/mL) of meplazumab, negative staining was found in 25 kinds of normal human tissues and 33 kinds of normal cynomolgus monkey tissues, and weak to moderate staining was observed in 7 kinds of human tissues, including the stomach (3/4 in parietal cells), kidney (1/3 in renal tubular epithelial cells), heart (1/3 in myocardial cells), liver (4/8 in hepatic cells), bladder (2/3 in urothelial cells), adrenal gland (2/3 in adrenal cortical epithelial cells) and prostate (2/3 in prostatic epithelial cells). In addition, CD31-positive staining was found in endothelial cells of all tissues (except for human spinal cord slices and human bone marrow smears, in which no endothelial cells were observed), indicating that the antigen was well preserved in all tissues; moreover, negative staining was found in all tissues in PBS blank control staining. In positive tissue control staining, positive membrane and cytoplasm staining in both human lung adenosquamous carcinoma tissues and human hepatocellular carcinoma tissues were observed after staining with meplazumab at low (1 μg/mL) and high (20 μg/mL) concentrations. Based on the above results, meplazumab had a low cross-reactivity rate in various tissues.

3.8. *Distribution and excretion in SD rats*

The individual tissue distribution of the TCA-precipitated peptide of ^{125}I-meplazumab in the rats is summarized in Fig. 3A. The

Table 3 Toxicokinetic parameters of ADA positive and ADA negative animals in cynomolgus monkeys in repeat-dose toxicity study.

Dose (mg/kg)	ADA	*n*	C_{max} (μg/mL)		$AUC_{0-168\ h}$ (μg·h/mL)	
			Mean ± SEM	CV%	Mean ± SEM	CV%
2	Negative	4	41.9 ± 9	22	1255 ± 391	31
	Positive	6	19.3 ± 8	42	120 ± 162	135
6	Negative	7	155.3 ± 29	19	6230 ± 847	14
	Positive	3	159.4 ± 7	4	3526 ± 1389	39
12	Negative	7	312.3 ± 44	14	19,768 ± 2626	13
	Positive	3	209.4 ± 160	76	54,644 ± 8523	156

ADA, anti-drug antibody; *n*, number of animal; the data of C_{max} and $AUC_{0-168\ h}$ was collected from the individuals during the first and fourth injection of meplazumab.

radioactive precipitation exposure $AUC_{0-240\ h}$ was highest in the plasma and lowest in the brain. Using radioactivity of precipitation to calculate the AUC, the AUC in each tissue was listed in the following order: plasma > whole blood > ovary > lung > blood cells > adrenal gland > liver > kidney > heart > mesentery lymph nodes > fat > spleen > femur > testis > intestine > thymus > stomach > urine > skeletal muscle > brain. As shown in Figs. 3B, ^{125}I-meplazumab underwent a rapid and widespread distribution in tissues throughout the whole body during the experiment. In most tissues and organs, the radiation concentration of ^{125}I-meplazumab reached its maximum distribution of 2 h after administration, and gradually decreased over time. At 240 h after administration, the radiation concentration of ^{125}I-meplazumab was mainly distributed in plasma, whole blood and blood cells (Fig. 3B). At each time point, the radiation concentration of ^{125}I-meplazumab in brain and skeletal muscle was very low, suggesting that meplazumab did not pass through the blood−brain barrier and did not accumulate in skeletal muscle tissue (Fig. 3B). The gamma counting results of different fractions of plasma and urine after HPLC separation showed that the corresponding peak of ^{125}I-meplazumab appeared at 10.3 min. No radioactive peak was observed from the urine at all-time points, indicating that the drug was mainly present as the form of metabolites in urine (HPLC data not provided). The total radiation content in the thyroid at 2 and 240 h after administration accounted for 0.08 ± 0.03% and 0.04 ± 0.02% of the radioactivity dose, respectively, indicating that ^{125}I-meplazumab did not accumulate in thyroid tissue.

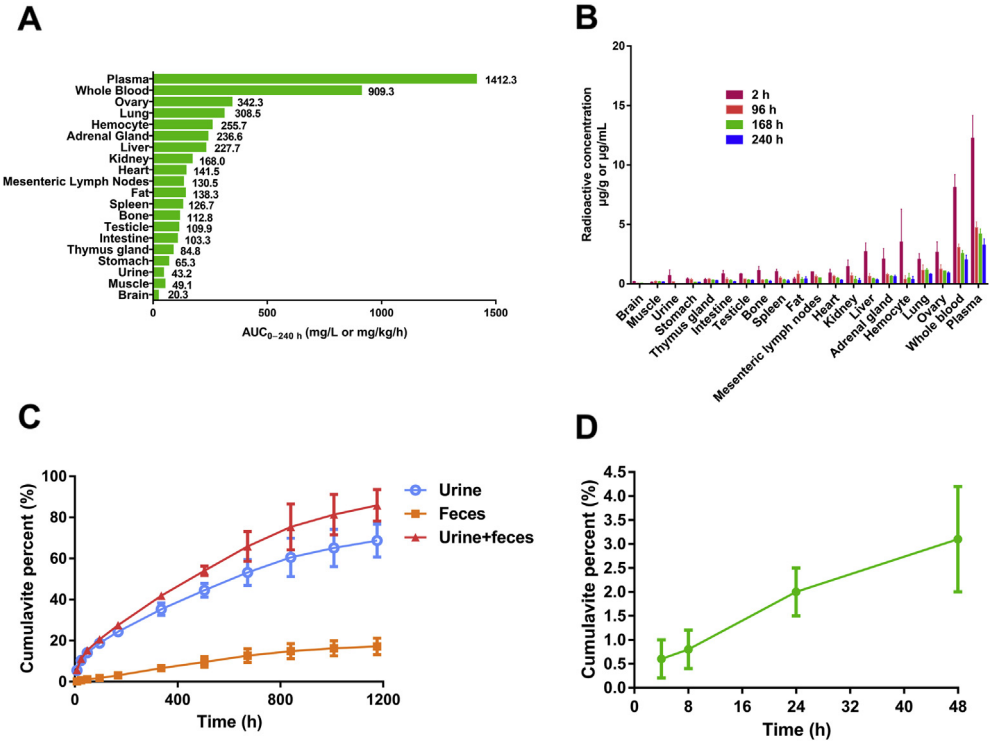

Figure 3 The radioactive precipitation distribution of ^{125}I-meplazumab in Sprague−Dawley rats. (A) The radioactive precipitation exposure $AUC_{0-240\ h}$ in the tissue/body fluid of Sprague−Dawley rats. (B) The radiation concentration of ^{125}I-meplazumab in tissues and organs of Sprague−Dawley rats at 2, 96, 168, and 240 h after administration. (C) The radiation detection results from the urine and feces of Sprague−Dawley rats within 1176 h after caudal vein injection with ^{125}I-meplazumab (mean ± SD). (D) The radiation detection results from the bile of Sprague−Dawley rats within 48 h after caudal vein injection with ^{125}I-meplazumab (mean ± SD).

A time course of the excreted radioactivity derived from ^{125}I-meplazumab in urine, feces, and bile is shown in Fig. 3C and D. Forty-eight hours after injection of ^{125}I-meplazumab, the excretory rates of radioactivity into the bile, urine and feces were 3.1 ± 1.1%, 14.1 ± 1.0%, and 1.2 ± 0.3%, respectively. At 1176 h, the excretory rates in the urine and feces were 68.7 ± 8.0% and 17.2 ± 4.0%, respectively, and the total excretory rate in the urine and feces was 85.9 ± 7.7%.

Based on these results, the radiolabeled drugs were mainly excreted by the urine and a small portion was eliminated in the feces.

3.9. *Activity of meplazumab against chloroquine-resistant strain Dd2 in huRBC-engrafted NOG mice*

Zhang et al.[19] confirmed the antimalarial efficacy of meplazumab on chloroquine-sensitive and -resistant *P. falciparum in vitro*. To further confirm that meplazumab also has a good therapeutic effect on drug-resistant strains of *P. falciparum in vivo*, we established a human erythrocyte chimeric NOG mouse model infected with *P. falciparum* Dd2 and evaluated the antimalarial efficacy of meplazumab in the constructed humanized mice. NOG mice were routinely observed after administration.

The results showed that compared with the human IgG group, parasitemia in the peripheral blood of mice treated with meplazumab ($P = 0.0031$) was significantly reduced (Fig. 4A and Supporting Information Table S15); compared with the chloroquine group, parasitemia in the peripheral blood of mice treated with meplazumab ($P = 0.0002$) was significantly reduced (Fig. 4A and Supporting Information Table S15). The chloroquine group had no significant inhibition after administration, while there was a significant difference between meplazumab and chloroquine on the parasite inhibition rate ($P < 0.0001$, Fig. 4B).

As shown in Supporting Information Table S16 and Fig 4C, 5 mg/kg meplazumab completely cleared malaria parasites from peripheral blood in humanized mice on Day 5, while chloroquine did not. The median parasite clearance time in the meplazumab group was significantly shorter than that of the human IgG group, with a PC_{50} value of 2.5 days ($P < 0.0001$). The PC_{50} of chloroquine was 7 days, and no significant difference was observed between chloroquine and human IgG ($P = 0.5188$).

3.10. *RO assays*

To determine the relationship between drug concentration and RO rate on erythrocytes after incubation of meplazumab with human peripheral blood and to provide reference for the initial dose in a clinical trial, RO% on erythrocytes after *in vitro* incubation of meplazumab with human peripheral blood was measured using flow cytometry. As shown in Fig. 5, the drug concentrations and the RO% were plotted to obtain a drug concentration−receptor occupancy level curve. The concentration of meplazumab at different RO rates was calculated from the model. Under the assumption of exclusively intravascular distribution and a blood volume of a healthy adult of approximately 77 mL/kg, meplazumab doses were projected. Maximum concentrations (C_{max}) required for a 10%, 20%, 50%, and 90% RO were determined and the corresponding projected doses were 0.511 ± 0.080, 0.820 ± 0.11, 1.634 ± 0.21 and 4.169 ± 0.71 μg/mL, respectively. When meplazumab exhibited intravascular distribution, the doses at the RO levels of 10%, 20%, 50% and 90% of C_{max} were predicted to be 39.3, 63.2, 125.8, and 321.0 μg/kg, respectively.

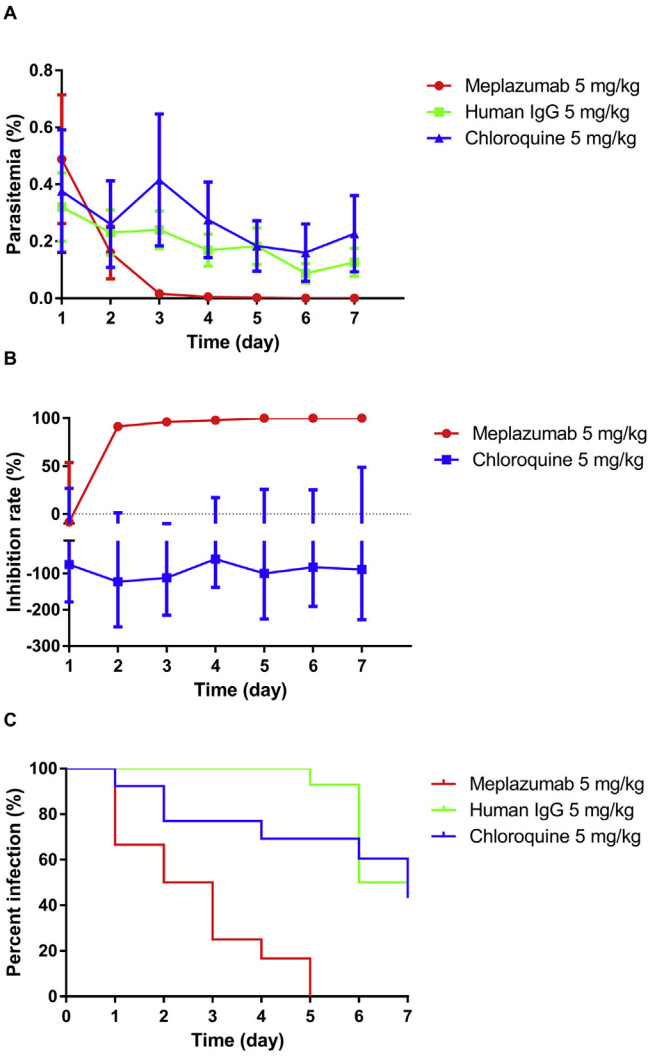

Figure 4 Antimalarial effect of meplazumab in huRBC chimeric NOG mice. (A) Parasitemia is shown as the proportion of erythrocytes infected with *P. falciparum* to total erythrocytes after administration. (B) The inhibition rate is shown as the inhibition ratio compared to the human IgG group after administration. (C) The parasite clearance−time curve in each group of mice. Levels are shown for the meplazumab group ($n = 5$−7), human IgG group ($n = 5$−9), and chloroquine group ($n = 6$−7). The results represent the mean ± SEM from two independent experiments.

4. Discussion

In recent years, increasing number of studies have shown that CD147 plays an important role in the invasion of erythrocytes by *P. falciparum*[19,35]. CD147 and its ligand proteins are becoming potential targets for antimalarial therapy[40,41]. Meplazumab is a humanized IgG2 mAb targeting human CD147 and is indicated for inhibitory prevention and treatment of *P. falciparum* infection. Repeat-dose toxicology studies of meplazumab have not been reported. To identify potential animal models for toxicology studies, we first determined the binding affinity of meplazumab to CD147 from different species. The results indicated that meplazumab could bind to CD147 from humans and cynomolgus monkeys. The affinity in humans is 13.5-fold higher than that in cynomolgus monkeys (Fig. 1A and B and Supporting Information

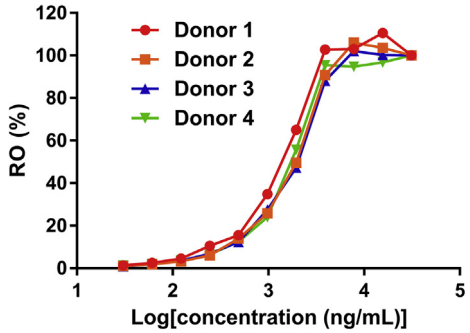

Figure 5 Concentration−receptor occupancy level curves of meplazumab. Peripheral venous blood samples were collected from four donors.

Table S1). The binding of meplazumab with RBCs of cynomolgus monkeys indicated that this species are appropriate for safety evaluation (Fig. 1C).

The repeat-dose toxicity and toxicokinetics of meplazumab were evaluated in cynomolgus monkeys after successive intravenous administration over 4 weeks with an interval of 1 week. The results demonstrated that meplazumab was well tolerated in the monkeys. No mortalities, significantly adverse reactions, or toxicities were observed in the treated animals. No changes in blood temperature, food consumption, or platelet counts were observed. No respiratory, cardiovascular, ophthalmological, or central nervous system impairments were noted in any of the treated animals. Increased percentage reticulocyte count dosed at >6 mg/kg was considered to be a pharmacodynamic effect, which should be used as an important indicator in clinical trials (Supporting Information Tables S7 and S8). No significant increase in exposure ($AUC_{0-168\ h}$) or accumulation of drug exposure was observed after 4 weeks of repeated intravenous administration (Table 1). No observed adverse effect level was estimated to be 12 mg/kg in monkeys.

ADA was detected in all surviving cynomolgus monkeys after repeat intravenous administration of meplazumab, and it may accelerate drug clearance and reduce exposure to drugs (Fig. 2E and F, and Table 3). However, the immunogenicity detection results depend largely on different factors, such as the type of assay, assay sensitivity, drug tolerance of the assay, drug administration route, time of sampling, and state of health. Furthermore, because of the species difference between humans and cynomolgus monkeys, the immunogenicity of meplazumab in the human body needs to be further studied in clinical trials[42].

The results of a normal human tissue cross-reactivity study showed that there was no cross-reactivity of meplazumab towards the lung, spleen, colon, small intestine or ovary. The tissues with a cross-reactivity rate of ≤20% included the liver, brain and testis. The tissues with a cross-reactivity rate of >20% included the heart and kidney (myocardial cells and renal tubular epithelial cells). This indicates that meplazumab has a low tissue cross-reactivity and high safety, and suggests that we should pay attention to the effect of meplazumab on the function of the human heart, kidney, etc. in clinical studies.

To evaluate the therapeutic potential of meplazumab, a study on the distribution and excretion of meplazumab was conducted in SD rats. Our data showed that meplazumab was mainly distributed in plasma, whole blood and blood cells making it more effective and specific in to clearing parasites in the blood. In addition, meplazumab did not pass through the blood–brain barrier and did not accumulate in skeletal muscle tissue. Meplazumab was mainly excreted by the urine.

A previous research confirmed that meplazumab blocked the interaction between CD147 and the RAP2 ligand, and inhibited the formation of parasitophorous vacuoles, thus blocking the route of *P. falciparum* to invade huRBCs, which is a different mechanism from other anti-falciparum malaria drugs[19]. Our results showed that meplazumab had no ADCC effect on human erythrocytes at concentrations up to 1 mg/mL. To some extent, it is confirmed that the antimalarial efficacy of meplazumab is to block the interaction between CD147 and RAP2 through Fab segment rather than ADCC activity of Fc segment. In addition, we established a chloroquine-resistant strain Dd2-infected humanized mouse model for the first time. Combined with previous studies[19,43,44], meplazumab at 5 mg/kg completely eliminated chloroquine-sensitive and -resistant parasites in humanized mice while chloroquine was ineffective against this resistant strain at 5 mg/kg, implicating that the efficacy of meplazumab is superior to that of chloroquine. Taken together, it is believed that meplazumab is an erythrocytic stage macromolecular antibody drug efficacious in the control of clinical occurrence and the inhibitory treatment of severe malaria.

5. Conclusions

In conclusion, the results from this study suggest that meplazumab is safe, tolerated, and effectively inhibits the chloroquine-resistant Dd2 strain of *P. falciparum* from invading huRBCs, and the efficacy was superior to that of chloroquine *in vivo*, which is promising as an efficacious drug for the cure of *P. falciparum*.

Acknowledgments

We thank Dr. Jing Ma, Dr. Yuanguo Cheng, Dr. Xi Zhu, and Dr. Yunliang Qiu from the National Shanghai Center for New Drug Safety Evaluation and Research (Shanghai InnoStar Bio-Tech Co., Ltd., Shanghai, China). We also thank Dr. Xiaochun Chen, Dr. Hao Tang, and Shuangshuang Liu from Jiangsu Pacific-Meinuoke Bio-pharmaceutical Co., Ltd. (Changzhou, China).

This work was supported by the National Science and Technology Major Project (2019ZX09732001, China) and the National Basic Research Program of China (2015CB553701, China).

Author contributions

Zhinan Chen, Ping Zhu, Huijie Bian, Zheng Zhang and Kun Zhang conceived and designed this study. Kun Zhang, Zheng Zhang, Yu Zhao performed experiments and analyzed the data. Mengyao Zhang and Xiaodong Wu performed partial experiments. Zhinan Chen, Ping Zhu and Huijie Bian drafted and revised the manuscript. The manuscript has been reviewed and approved by all authors.

Conflicts of interest

The authors have declared that no conflicts of interest exist.

Appendix A. Supporting information

Supporting data to this article can be found online at https://doi.org/10.1016/j.apsb.2020.06.011.

References

1. World Health Organization. *World malaria report 2019*. World Health Organization; 2019. Available from: https://www.who.int/publications-detail/world-malaria-report-2019.
2. Banda CG, Chaponda M, Mukaka M, Mulenga M, Hachizovu S, Kabuya JB, et al. Efficacy and safety of artemether-lumefantrine as treatment for *Plasmodium falciparum* uncomplicated malaria in adult patients on efavirenz-based antiretroviral therapy in Zambia: an open label non-randomized interventional trial. *Malar J* 2019;**18**:180.
3. Ghimire P, Rijal KR, Kafle C, Karki BS, Singh N, Ortega L, et al. Efficacy of artemether-lumefantrine for the treatment of uncomplicated *Plasmodium falciparum* malaria in Nepal. *Trop Dis Travel Med Vaccines* 2018;**4**:9.
4. Anthony MP, Burrows JN, Duparc S, Moehrle JJ, Wells TN. The global pipeline of new medicines for the control and elimination of malaria. *Malar J* 2012;**11**:316.
5. Fehintola FA, Adedeji AA, Gbotosho GO, Happi CT, Balogun ST, Folarin OA, et al. Effects of artesunate-cotrimoxazole and amodiaquine-artesunate against asexual and sexual stages of *Plasmodium falciparum* malaria in Nigerian children. *J Infect Chemother* 2008;**14**:188−94.
6. Sekihara M, Tachibana SI, Yamauchi M, Yatsushiro S, Tiwara S, Fukuda N, et al. Lack of significant recovery of chloroquine sensitivity in *Plasmodium falciparum* parasites following discontinuance of chloroquine use in Papua New Guinea. *Malar J* 2018;**17**:434.
7. Young MD. Failure of chloroquine and amodiaquine to suppress *Plasmodium falciparum*. *Trans R Soc Trop Med Hyg* 1962;**56**:252−6.
8. Young MD, Moore DV. Chloroquine resistance in *Plasmodium falciparum*. *Am J Trop Med Hyg* 1961;**10**:317−20.
9. World Health Organization. *Guidelines for the treatment of malaria*. 3rd ed. World Health Organization; 2015. Available from: https://www.who.int/malaria/publications/atoz/9789241549127/en/.
10. Fidock DA, Nomura T, Talley AK, Cooper RA, Dzekunov SM, Ferdig MT, et al. Mutations in the *P. falciparum* digestive vacuole transmembrane protein PfCRT and evidence for their role in chloroquine resistance. *Mol Cell* 2000;**6**:861−71.
11. Ecker A, Lehane AM, Clain J, Fidock DA. PfCRT and its role in antimalarial drug resistance. *Trends Parasitol* 2012;**28**:504−14.
12. Foote SJ, Kyle DE, Martin RK, Oduola AM, Forsyth K, Kemp DJ, et al. Several alleles of the multidrug-resistance gene are closely linked to chloroquine resistance in *Plasmodium falciparum*. *Nature* 1990;**345**:255−8.
13. Duraisingh MT, Cowman AF. Contribution of the *pfmdr1* gene to antimalarial drug-resistance. *Acta Trop* 2005;**94**:181−90.
14. Ibraheem ZO, Abd MR, Noor SM, Sedik HM, Basir R. Role of different *Pfcrt* and *Pfmdr-1* mutations in conferring resistance to antimalaria drugs in *Plasmodium falciparum*. *Malar Res Treat* 2014;**2014**:950424.
15. Adam I, Ibrahim Y, Gasim GI. Efficacy and safety of artemisinin-based combination therapy for uncomplicated *Plasmodium falciparum* malaria in Sudan: a systematic review and meta-analysis. *Malar J* 2018;**17**:110.
16. Chakrabarti R, White J, Babar PH, Kumar S, Mudeppa DG, Mascarenhas A, et al. Decreased *in vitro* artemisinin sensitivity of *Plasmodium falciparum* across India. *Antimicrob Agents Chemother* 2019;**63**:e00101−19.
17. Ouji M, Augereau JM, Paloque L, Benoit-Vical F. *Plasmodium falciparum* resistance to artemisinin-based combination therapies: a sword of Damocles in the path toward malaria elimination. *Parasite* 2018;**25**:24.
18. Laurens MB. The promise of a malaria vaccine—are we closer?. *Annu Rev Microbiol* 2018;**72**:273−92.
19. Zhang MY, Zhang Y, Wu XD, Zhang K, Lin P, Bian HJ, et al. Disrupting CD147−RAP2 interaction abrogates erythrocyte invasion by *Plasmodium falciparum*. *Blood* 2018;**131**:1111−21.
20. Mehnert JM, Varga A, Brose MS, Aggarwal RR, Lin CC, Prawira A, et al. Safety and antitumor activity of the anti-PD-1 antibody pembrolizumab in patients with advanced, PD-L1-positive papillary or follicular thyroid cancer. *BMC Canc* 2019;**19**:196.
21. Bykerk VP. Adalimumab for early rheumatoid arthritis. *Expet Rev Clin Immunol* 2008;**4**:157−63.
22. Dhillon S. Obinutuzumab: a review in rituximab-refractory or -relapsed follicular lymphoma. *Targeted Oncol* 2017;**12**:255−62.
23. Overdijk MB, Verploegen S, Bogels M, van Egmond M, Lammerts van Bueren JJ, Mutis T, et al. Antibody-mediated phagocytosis contributes to the anti-tumor activity of the therapeutic antibody daratumumab in lymphoma and multiple myeloma. *mAbs* 2015;**7**:311−21.
24. Lyu H, Han A, Polsdofer E, Liu S, Liu B. Understanding the biology of HER3 receptor as a therapeutic target in human cancer. *Acta Pharm Sin B* 2018;**8**:503−10.
25. FDA. *Safety reporting requirements for INDs and BA/BE studies*. USA. 19 December 2012. Available from: https://www.fda.gov/media/79394/download.
26. Talamonti M, Spallone G, Di Stefani A, Costanzo A, Chimenti S. Efalizumab. *Expet Opin Drug Saf* 2011;**10**:239−51.
27. Jakobsen JN, Urup T, Grunnet K, Toft A, Johansen MD, Poulsen SH, et al. Toxicity and efficacy of lomustine and bevacizumab in recurrent glioblastoma patients. *J Neuro Oncol* 2018;**137**:439−46.
28. Hahn VS, Lenihan DJ, Ky B. Cancer therapy-induced cardiotoxicity: basic mechanisms and potential cardioprotective therapies. *J Am Heart Assoc* 2014;**3**:e000665.
29. Weber JS, Kahler KC, Hauschild A. Management of immune-related adverse events and kinetics of response with ipilimumab. *J Clin Oncol* 2012;**30**:2691−7.
30. Chapman K, Pullen N, Graham M, Ragan I. Preclinical safety testing of monoclonal antibodies: the significance of species relevance. *Nat Rev Drug Discov* 2007;**6**:120−6.
31. Dixit R, Boelsterli UA. Healthy animals and animal models of human disease(s) in safety assessment of human pharmaceuticals, including therapeutic antibodies. *Drug Discov Today* 2007;**12**:336−42.
32. Roberts R, McCune SK. Animal studies in the development of medical countermeasures. *Clin Pharmacol Ther* 2008;**83**:918−20.
33. Zhang Z, Tang W. Drug metabolism in drug discovery and development. *Acta Pharm Sin B* 2018;**8**:721−32.
34. Muramatsu T. Basigin (CD147), a multifunctional transmembrane glycoprotein with various binding partners. *J Biochem* 2016;**159**:481−90.
35. Crosnier C, Bustamante LY, Bartholdson SJ, Bei AK, Theron M, Uchikawa M, et al. Basigin is a receptor essential for erythrocyte invasion by *Plasmodium falciparum*. *Nature* 2011;**480**:534−7.
36. Volz JC, Yap A, Sisquella X, Thompson JK, Lim NT, Whitehead LW, et al. Essential role of the PfRh5/PfRipr/CyRPA complex during *Plasmodium falciparum* invasion of erythrocytes. *Cell Host Microbe* 2016;**20**:60−71.
37. Zhang Z, Zhang Y, Sun Q, Feng F, Huhe M, Mi L, et al. Preclinical pharmacokinetics, tolerability, and pharmacodynamics of metuzumab, a novel CD147 human-mouse chimeric and glycoengineered antibody. *Mol Canc Therapeut* 2015;**14**:162−73.
38. Milligan C, Richardson BA, John-Stewart G, Nduati R, Overbaugh J. Passively acquired antibody-dependent cellular cytotoxicity (ADCC) activity in HIV-infected infants is associated with reduced mortality. *Cell Host Microbe* 2015;**17**:500−6.
39. Ernst D, Williams BA, Wang XH, Yoon N, Kim KP, Chiu J, et al. Humanized anti-CD123 antibody facilitates NK cell antibody-dependent cell-mediated cytotoxicity (ADCC) of Hodgkin lymphoma targets *via* ARF6/PLD-1. *Blood Canc J* 2019;**9**:6.

40. Drew DR, Beeson JG. PfRH5 as a candidate vaccine for *Plasmodium falciparum* malaria. *Trends Parasitol* 2015;**31**:87−8.
41. Zenonos ZA, Dummler SK, Muller-Sienerth N, Chen J, Preiser PR, Rayner JC, et al. Basigin is a druggable target for host-oriented antimalarial interventions. *J Exp Med* 2015;**212**:1145−51.
42. Ponce R, Abad L, Amaravadi L, Gelzleichter T, Gore E, Green J, et al. Immunogenicity of biologically-derived therapeutics: assessment and interpretation of nonclinical safety studies. *Regul Toxicol Pharmacol* 2009;**54**:164−82.
43. Angulo-Barturen I, Jimenez-Diaz MB, Mulet T, Rullas J, Herreros E, Ferrer S, et al. A murine model of falciparum-malaria by *in vivo* selection of competent strains in non-myelodepleted mice engrafted with human erythrocytes. *PloS One* 2008;**3**:e2252.
44. Jimenez-Diaz MB, Mulet T, Viera S, Gomez V, Garuti H, Ibanez J, et al. Improved murine model of malaria using *Plasmodium falciparum* competent strains and non-myelodepleted NOD-scid IL2Rgammanull mice engrafted with human erythrocytes. *Antimicrob Agents Chemother* 2009;**53**:4533−6.